
Transmitting phase-aligned signals for array steering with USRPs X310

C. Campo⁽¹⁻²⁾

CLEMENT.CAMPO@ISL.EU

French-German research Institute of Saint-Louis (ISL), 5 rue du général Cassagnou, Saint-Louis 68300, France

L. Bernard⁽¹⁾, H. Boeglen⁽²⁾, S. Hengy⁽¹⁾, J.-M. Paillot⁽²⁾

HERVE.BOEGLLEN@UNIV-POITIERS.FR

(1): French-German research Institute of Saint-Louis (ISL), 5 rue du général Cassagnou, Saint-Louis 68300, France

(2): XLIM laboratory, university of Poitiers, F-86000 Poitiers, France.

Abstract

More affordable commercial systems and high reconfigurability have made Software-Defined Radios (SDR) a serious candidate for many complex radio systems. This work is part of a study that investigates the usability of the commercial Universal Software Radio Peripheral (USRP) for antenna array steering applications, which require all signals to be phase synchronized. The following details the specific problems met when the steered array transmits signals, draws the comparison with the previous work that focused on steering a receiving array, and presents the proposed solution to automate phase synchronization between the different transmitting channels. The radiation patterns of two four-element Uniform Linear Arrays (ULA) are measured after calibration as a result.

1. Introduction and problem

Cost reduction, as well as the flexibility offered by using programmable components functional over a large frequency range and moving some of the signal processing to software, have made Software-Defined Radio (SDR) an economically viable technology for developing many “intelligent” radio systems, such as mobile telephony base stations (Perez-Neira et al., 2001). Among the numerous applications SDR can be used for, array steering remains specific as it also requires the signals of all array elements to be synchronized in phase (Balanis, 2005).

In this work, two National Instruments’ Universal Software Radio Peripherals (USRPs) X310 (Ettus, 2014) are equipped with two UBX-160 daughterboards (Ettus, 2015) each and synchronized using an Octoclock-G (Ettus, b). The main difficulty when trying to steer antenna arrays with

commercial USRPs is that, despite them being synchronized in both time and frequency by 1-PPS and 10 MHz clock signals respectively, only the converters are synchronized in time. The Phase-Locked Loops (PLLs) are synchronized in frequency but are initialized with a random phase, hence random phase shifts are introduced between the signals of each channel. The frequency synchronization provides phase coherence (Ettus, 2016) but random phase shifts that change with each power-up cycle prevent the system from achieving the required phase alignment between channels to effectively steer antenna arrays. In order to enable array steering applications with USRPs, phase synchronization needs to be carried out by the user before each measurement (Krueckemeier et al., 2019).

This work follows previous studies that focused on steering receiving antenna arrays after synchronizing USRPs in phase (Campo et al., 2017) and related applications, such as passive tracking of a transmitting projectile (Campo et al., 2021). The objective in these previous studies (and in this work too) was to explore the USRP limitations with regard to array steering applications. Hence, when looking to perform phase calibration between channels, priority is always given to solutions which require the least possible additional hardware. Within that frame of mind, phase calibration was carried out only in software for receiving applications. For this transmitting application however, an additional RF phase calibration circuit has been added to the existing commercial equipment to enable phase-aligned applications. The problem caused by phase synchronization between channels is compared for receiving and transmitting applications in Fig. 1 and is detailed in the next paragraphs.

Indeed, Fig. 1 shows that USRP reception and transmission conversion chains introduce random phase shifts between n channels, noted TX_i or RX_j for the i^{th} transmission or j^{th} reception channel respectively ($1 \leq i, j \leq n$). Fig. 1a shows the case which previous studies focused on, i.e. the array steered by USRPs is used as a receiver. If the transmitter is aligned with the perpendicular to the array axis, planar wavefronts reach all array elements at the same mo-

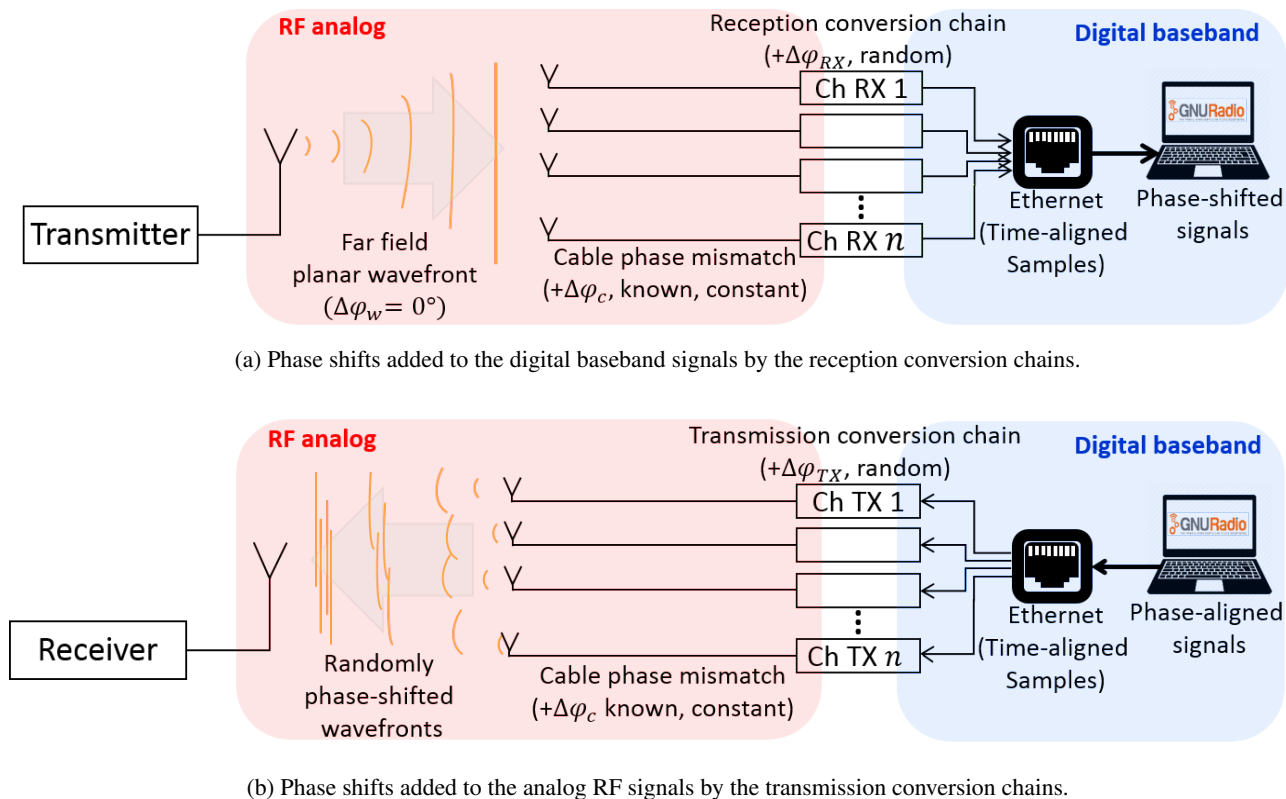


Figure 1. Issue related to random phase shifts between channels for transmitting applications compared to receiving ones.

ment but the random phase shifts introduced by conversion chains are responsible for the observed phase-shifted signals in the digital baseband. In that case, the phase shifts between the digitized signals can be measured while the transmitter is aligned with the array. They can then be compensated in software for the entire measurement, ensuring that the phase shifts induced by moving the transmitter or steering the array remain uncorrupted by analog-to-digital conversion. This solution enables array steering for receiving applications with USRPs with no need for any additional hardware.

On the other hand, Fig. 1b presents the case where the steered array transmits signals at the carrier frequency to each array element based on a digital baseband signal. Although the same digital baseband signal feeds each transmission channel, the transmission conversion chains introduce random phase shifts between the n generated RF analog signals. As in the previous case, these phase shifts prevent the array element signals from interfering constructively and no radiation pattern can be formed using the USRPs. In the case of a one-way transmission however, a priori knowledge on the receiver position does not allow to measure and compensate these random phase shifts directly in software. Hence, the used commercial equipment based on USRPs X310 appears unable to steer transmitting

antenna arrays.

2. Proposed solution

Previous studies highlighted a first limitation of the commercial equipment with regard to phase-aligned applications. This limitation was overcome in the case of a receiving array by performing a phase calibration in specific conditions before measurement. The USRPs then proved suitable for steering a receiving array if the constraint of knowing the transmitter position prior to measurement was compatible with the application. The problem presented in the previous section brings to light another limitation of this equipment when the array to be steered is a transmitter, as phase calibration cannot be carried out with only the USRPs. The proposed calibration circuit consists in looping the transmitted RF analog signals to receiving channels and use the previous study results to enable phase calibration between the transmitting channels. Fig. 2 shows the resulting circuit.

The calibration circuit is placed between the USRPs (symbolized by their conversion chains) and the antenna array. During phase calibration, transmitted signals are looped to two reception channels $RX1$ and $RX2$, independently of the number of transmitting channels, so that images of the

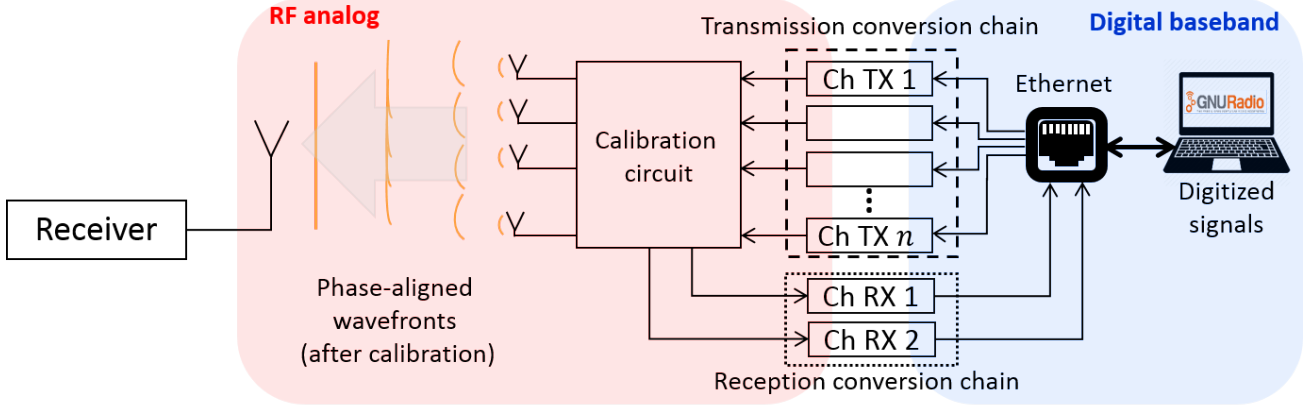


Figure 2. Proposed setup to steer a transmitting array after phase calibrating the USRPs.

transmitted signals can be visualized in the digital baseband. The digitized signal obtained from $RX1$ is always the image of the signal transmitted on $TX1$, arbitrarily chosen as the phase reference, while $RX2$ is used to visualize an image of any of the n transmitting channels. Phase shifts between these images of the transmitted signals are then measured in software. By isolating the phase shifts introduced by the transmission conversion chains, the system can be calibrated. But the previous section explained that the reception conversion chains, which are used to visualize images of the transmitted signals, also introduce random phase shifts. Hence, a multiple-step calibration algorithm is implemented in GNU Radio in order to isolate the phase shifts introduced by each conversion chain. The calibration circuit is only made of passive RF components. Its phase response remains constant at a known carrier frequency and is measured beforehand, so its influence does not appear in the following equations but is taken into account in the implemented algorithm. Let us consider an analog baseband signal s carrying the information to be transmitted. \tilde{s} is the complex envelope of s and s_{BB} is the corresponding digital IQ signal available in GNU Radio. It is supposed that conversion chains only phase shift signals but do not distort them, i.e. s can be retrieved from s_{BB} and vice-versa.

s_{BB} is converted to the analog domain at carrier frequency f_c through the i^{th} transmitting channel TXi , is looped using the calibration circuit and converted back to the digital baseband through the j^{th} receiving channel RXj . The random phase shifts brought by the conversion chains are noted ϕ . The resulting setup is summarized in Fig. 3. The transmitted signal and its received image in the digital baseband are described by Eqs. 1 and 2 respectively.

$$s_{TXi}(t) = \Re(\tilde{s}(t) e^{j2\pi f_c t} e^{j\phi_{TXi}}) \quad (1)$$

$$s_{RXj} = s_{BB} e^{j\phi_{TXi}} e^{j\phi_{RXj}} \quad (2)$$

From Eq. 2, it is clear the random phase shift ϕ_{RXj} must be first isolated and compensated before ϕ_{TXi} can be properly measured. In order to remove ϕ_{RXj} from the equation, the signal transmitted on the first channel $TX1$ is looped simultaneously on both $RX1$ and $RX2$ using a power splitter. Since both reception conversion chains sample at the same time, the phase shift α_{12} introduced between the two images of the transmitted signal can be computed, as shown in Eq 3.

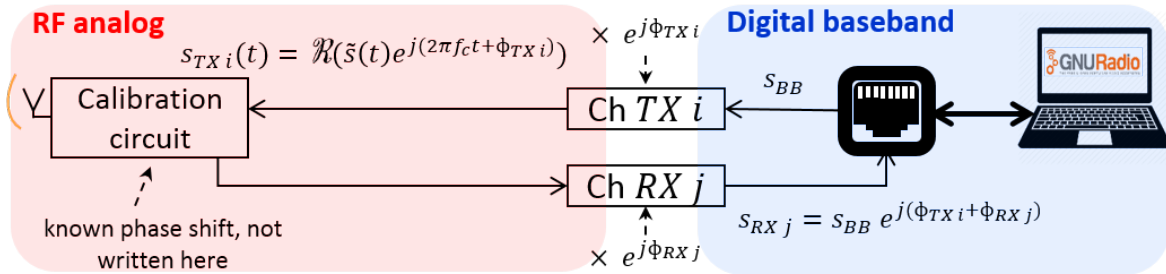


Figure 3. Random phase shifts added to the received image of a transmitted signal.

$$\frac{s_{RX1}}{s_{RX2}} = \frac{0.5 s_{BB} e^{j\phi_{TX1}} e^{j\phi_{RX1}}}{0.5 s_{BB} e^{j\phi_{TX1}} e^{j\phi_{RX2}}} = \frac{e^{j\phi_{RX1}}}{e^{j\phi_{RX2}}} = \alpha_{12} \quad (3)$$

Once α_{12} is known, the phase shift β_{1i} introduced by the transmission conversion chains between the first and the i^{th} channels can be computed in software using Eq. 4.

$$\frac{s_{RX1}}{\alpha_{12} s_{RX2}} = \frac{e^{j\phi_{RX2}} s_{BB} e^{j\phi_{TX1}} e^{j\phi_{RX1}}}{e^{j\phi_{RX1}} s_{BB} e^{j\phi_{TX1}} e^{j\phi_{RX2}}} = \frac{e^{j\phi_{TX1}}}{e^{j\phi_{TXi}}} = \beta_{1i} \quad (4)$$

By repeating this process for all transmitting channels from the second to the n^{th} , all phases can be aligned to that of the reference $TX1$. After calibration, the baseband digital signal $s_{BB \text{ cal } i}$ feeds the i^{th} transmitting channel, as shown in Eq. 5.

$$s_{BB \text{ cal } i} = \beta_{1i} s_{BB} \quad (5)$$

Using Eqs. 1 and 5, the expression of the i^{th} transmitted analog signal becomes s'_{TXi} , which is described by Eq. 6.

$$\begin{aligned} s'_{TXi}(t) &= \Re(\beta_{1i} \tilde{s}(t) e^{j2\pi f_c t} e^{j\phi_{TXi}}) \\ &= \Re(\tilde{s}(t) e^{j2\pi f_c t} e^{j\phi_{TX1}}) \end{aligned} \quad (6)$$

Eq. 6 shows the expression of the i^{th} transmitted signal does not depend on i anymore, allowing phase alignment for the USRPs. In the end, the implemented algorithm takes into account the computed values β_{1i} as well as the known

phase shifts introduced by the calibration circuit at the carrier frequency.

It can be noted that the described calibration procedure compensates the random phase offsets introduced by the tuning of the PLLs, which occurs every time the system is power-cycled or tuned to a different carrier frequency. As long as the PLLs remain tuned, phase offsets remain constant independently from any datastream or signal processing carried out in software. Depending on the equipment used, timed-tuning commands can be used in Python to tune multiple frontends at a specific time, ensuring phase offsets remain constant after the PLLs are re-tuned (Ettus, a). However, a part of the phase offsets between channels is introduced by components such as mixers, amplifiers, etc, which responses vary with time and temperature (Ettus, 2016). Hence, phase drift is to be expected over time and periodic calibration remains mandatory. The presented solution allows for an automated periodic calibration that can be set by the user in software for different carrier frequencies and independently from the receiver position.

3. Experimental results

The proposed calibration solution is meant to enable steering of transmitting antenna arrays. The algorithm presented in the previous section is implemented in a GNU Radio block named *Full calibration TX*. The resulting GNU Radio flowgraph is shown in Fig. 4. Signals are converted to the analog domain through four channels $TX1$ to $TX4$, accessed via the *USRP Sink* block (purple). The looped signals are accessed using the *USRP Source* block (blue). Images of the transmitted signals are compared using Eqs. 3 and 4 in the *Full calibration TX* block (gray). Once the

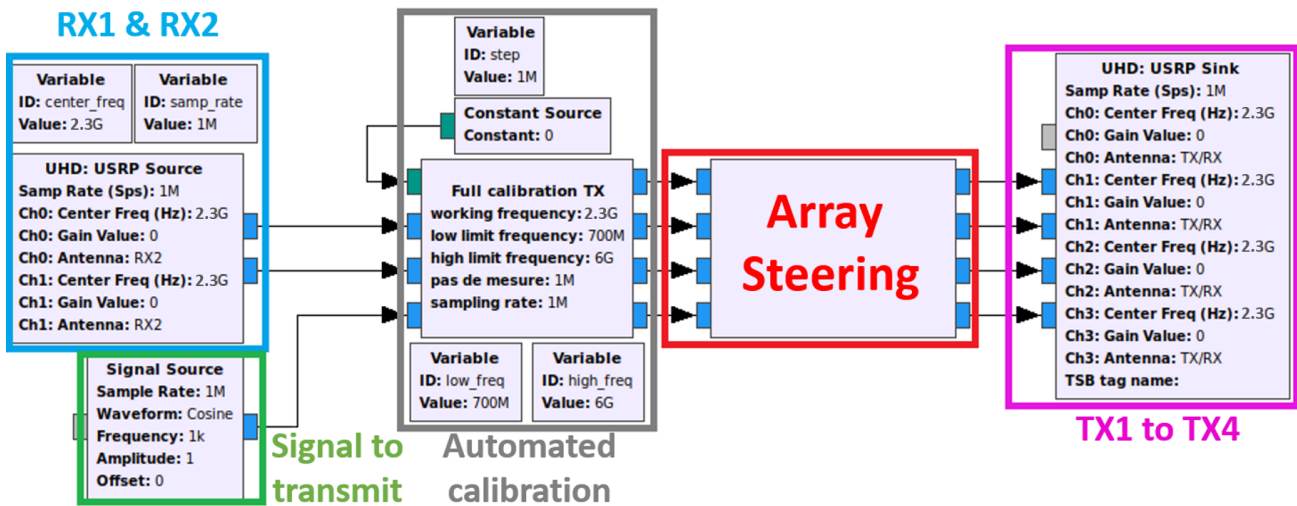


Figure 4. GNU Radio program used to calibrate and steer a four-element transmitting ULA

values of β_{1i} are known, the phase-shifted signals s'_{TXi} of Eq. 6 can be accessed via the *Full calibration TX* block outputs. Any implemented array steering function (red) can be applied to the calibrated signals. The remaining of this paper uses a beamsteering block to steer the array main lobe in a direction θ chosen by the user.

Experimental validation is done by measuring the radiation patterns of two Uniform Linear Arrays (ULAs) that were designed at ISL. The ULAs have four elements each, and are optimized to work at 2.3 GHz (Bernard & Jaeck, 2013) and 3.1 GHz carrier frequencies respectively. Their radiation patterns are measured when steered by USRPs using the flowgraph presented in Fig. 4. These radiation patterns are compared to the array factor (AF) of a four element ULA in Fig. 5. Good agreement is found between the simulated array factor and the measured radiation patterns, as a main lobe and two sidelobes can be observed in each case. The direction of the main lobe, which is determined by the phase relation between all element signals, matches within a few degrees, showing phase shifts between signals have been significantly reduced. Divergences between the simulated and measured plots can be attributed to the array factor not taking into account each element individual radiation pattern, and measurement approximations such as misalignment between the transmitter and the receiver.

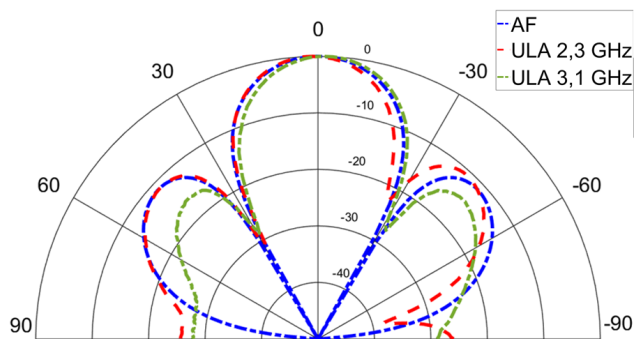


Figure 5. Comparison between a 4-element ULA array factor and the measured radiation patterns.

The main lobe of the ULA designed to work at a 2.3 GHz carrier frequency is then steered towards a direction θ in the angular range $[-30^\circ; +30^\circ]$. The resulting radiation patterns obtained for all values of θ are displayed in Fig. 6.

Fig. 6 shows the array main lobe is effectively steered towards the direction set by the user, confirming the proposed system is suitable for transmitting array steering applications. The error between the user order in software and the angle corresponding to the maximum of the measured radiation pattern remains inferior to $\pm 3^\circ$ for all tested values of θ in the angular range $[-30^\circ; +30^\circ]$, which is acceptable considering the ULA Half Power Beam Width (HPBW) is 26° .

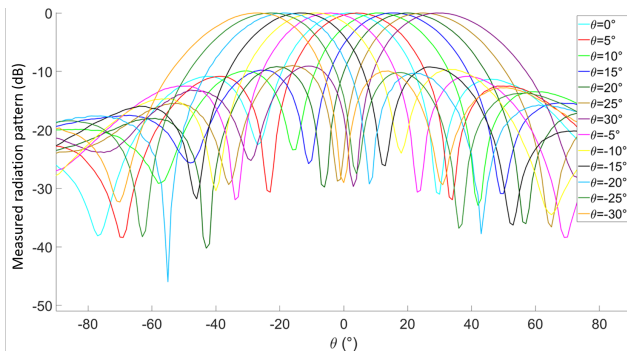


Figure 6. Measured radiation patterns of the 4-element ULA for different main lobe direction orders θ .

Conclusion

This work is part of a study which highlights the capabilities and limitations of the commercial Ettus X310 with regard to phase-aligned applications. As the equipment uses PLLs to synchronize the different channels in frequency but not in phase, it enables phase coherence but requires the user to handle phase calibration procedures to achieve phase alignment. A previous work demonstrated that phase alignment can be achieved between receiving channels by performing an automated calibration in software if the transmitter is aligned with the receiving antenna array, enabling phase-aligned operating. However, when the array is used as a transmitter this software solution cannot isolate the random phase shifts that need to be compensated. In order to alleviate this limitation, an additional RF circuit is introduced between the USRP transmission conversion chains and the antenna array to loop the transmitted RF signals back to receiving channels. Images of the transmitted signals can then be visualized in software and previous results can be used to isolate the phase shifts induced only by the transmission conversion chains.

A first experimental result demonstrates the proposed system ability to align the phases of all transmitting channels by measuring radiation patterns for two ULAs of four elements, at 2.3 GHz and 3.1 GHz carrier frequencies respectively. Finally, radiation patterns of the first ULA are shown for directions of the array main lobe θ set in the angular range $[-30^\circ; +30^\circ]$. For all values of θ , the error between the order given by the user and the measured maximum of the array main lobe is found to be within $\pm 3^\circ$, proving the system can steer the antenna array. Further details on the proposed system and array steering measurements will be provided in the full presentation.

References

Balanis, Constantine A. *Antenna Theory: Analysis and Design*. Wiley-Interscience, New York, NY, USA, 2005.

ISBN 0471714623.

Bernard, L. and Jaeck, V. Investigations on bandwidth enhancement of low cost printed phased array with reactive impedance substrates. In *2013 IEEE International Symposium on Phased Array Systems and Technology*, pp. 279–284, Oct 2013. doi: 10.1109/ARRAY.2013.6731842.

Campo, C., Stefer, M., Bernard, L., Hengy, S., Boeglen, H., and M. Paillot, J. Antenna Weighting System for a Uniform Linear Array based on Software Defined Radio. In *2017 Mediterranean Microwave Symposium (MMS)*, pp. 1–4, Nov 2017. doi: 10.1109/MMS.2017.8497138.

Campo, C., Boeglen, H., Paillot, J. M., Bieber, É., Hengy, S., and Bernard, L. Software-defined radio based station for projectile tracking and telemetry reception enhancement. *IEEE Transactions on Aerospace and Electronic Systems*, 57(2):1057–1068, 2021. doi: 10.1109/TAES.2020.3042621.

Ettus. USRP and hardware driver manual. https://files.ettus.com/manual/page_sync.html, a.

Ettus. Octoclock CDA-2990 time and frequency reference distribution device. https://kb.ettus.com/OctoClock_CDA-2990, b.

Ettus. USRP X310. <https://kb.ettus.com/X300/X310>, 2014.

Ettus. UBX-160 daughterboard for USRP X310. <https://www.ettus.com/all-products/ubx160/>, 2015.

Ettus. Synchronization and MIMO Capability with USRP devices. https://kb.ettus.com/Synchronization_and_MIMO_Capability_with_USRP_Devices, 2016.

Krueckemeier, M., Schwartau, F., Monka-Ewe, C., and Technische, J. S. Synchronization of Multiple USRP SDRs for Coherent Receiver Applications. In *2019 Sixth International Conference on Software Defined Systems (SDS)*, pp. 11–16, 2019. doi: 10.1109/SDS.2019.8768634.

Perez-Neira, A., Mestre, X., and Fonollosa, J. R. Smart antennas in software radio base stations. *IEEE Communications Magazine*, 39(2):166–173, 2001.